EXOTICS SEARCHES WITH ATLAS AND CMS EXPERIMENTS*

Santiago González de la Hoz

on behalf of the ATLAS and CMS collaborations

IFIC, Instituto de Física Corpuscular
Centro Mixto Universitat de València — CSIC, Parque científico
C/Catedrático José Beltrán, 2, 46980 Paterna (Valencia), Spain

(Received April 15, 2014)

In this paper, we present strategies and results of nine searches for exotic physics performed by the ATLAS and CMS experiments with 2012 pp collision data taken at LHC energy $\sqrt{s} = 7$ TeV and 8 TeV. Among them, there are searches from one object to many objects in the final state covering mono-X, two leptons, two jets, photon+X, microscopic black holes, dibosons, $t\bar{t}$ resonances and vector-like top quark analyses.

DOI:10.5506/APhysPolB.45.1371
PACS numbers: 12.60.–i, 13.85.Rm

1. Introduction

The Standard Model (SM) of elementary particles is a very successful theory with precise predictions verified by experiments over many orders of magnitude. The searches for physics Beyond the Standard Model (BSM) are one of the main goals of the experiments [1, 2] at the Large Hadron Collider (LHC). These searches are traditionally divided in two main groups: searches for Supersymmetry (SUSY) and non-SUSY searches. The latter is usually referred to as searches for exotics. It includes not only theories and models very different from SUSY, like extra dimensions and quark and lepton compositeness, but also special cases of SUSY.

2. Searches for mono-X in the final state

Events with an energetic jet of hadrons and large missing momentum in the final state constitute a clean and distinctive signature in searches for

* Presented at the Cracow Epiphany Conference on the Physics at the LHC, Kraków, Poland, January 8–10, 2014.

new physics at colliders. In particular, mono-jet and mono-W/Z final states have been studied in the context of searches for supersymmetry (gravitinos), large extra spatial dimensions (LED) aiming to provide a solution to the mass hierarchy problem, and the search for weakly interacting massive particles (WIMPs) as candidates for dark matter (DM). The Arkani-Hamed, Dimopoulos, and Dvali (ADD) model for LED explains the large difference between the electroweak unification scale $O(10^2)$ GeV, and the Planck scale $M_{\mathrm{Pl}} \sim O(10^{19})$ GeV by postulating the presence of n extra dimensions of size R, and defining a fundamental Planck scale in $4 + n$ dimensions, M_D, given by $M_{\mathrm{Pl}}^2 \sim M_D^{2+n} R^n$. An appropriate choice of R for a given n yields to a value of M_D at the electroweak scale.

In the case of mono-jet searches in pp collisions at $\sqrt{s} = 8$ TeV at the LHC, events with an energetic jet and large missing transverse momentum have been analyzed using 10.5 fb^{-1} of ATLAS data and 19.5 fb^{-1} of CMS data [3, 4]. Figure 1 shows that the measurements are in agreement with the SM predictions for the background. The results were translated into model-independent 95% confidence level (C.L.) upper limits on the production cross section times acceptance times efficiency ($\sigma \times A \times \epsilon$). The results were also presented in terms of new limits on the production of light gravitinos in association with gluinos or scalar quarks in a gauge-mediated supersymmetric model, leading to the best lower bound to date on the gravitino mass. In addition, 95% C.L. limits on M_D *versus* the number of extra spatial dimensions, in the ADD LED model, and on the suppression scale M_* *versus*

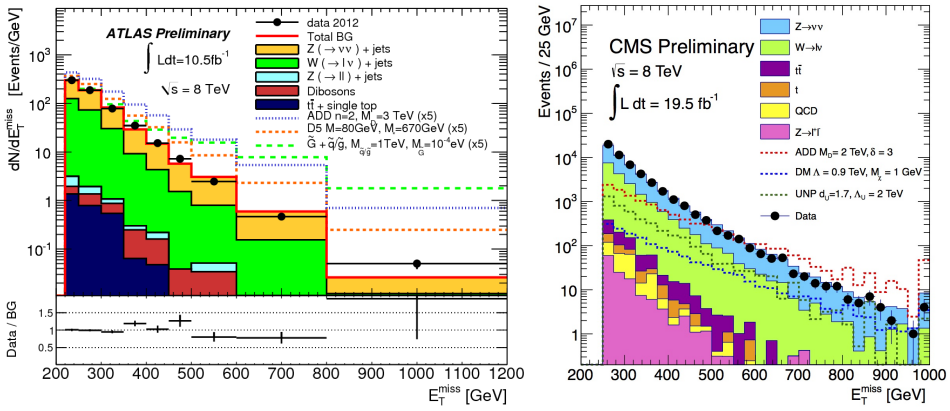

Fig. 1. Measured missing transverse momentum $E_{\mathrm{T}}^{\mathrm{miss}}$ distributions (black dots in the upper plot) in the signal region compared to the predictions for SM backgrounds (histograms). For illustration purposes, the impact of different ADD, WIMPS, and GMSB scenarios are included for ATLAS (left) [3], and dark matter ADD and unparticles are overlaid for the CMS (right) [4].

the WIMP mass, for the pair production of dark matter candidates, were presented that only partially supersede previous results. These constraints were an improvement over previous results as it is shown in Fig. 2.

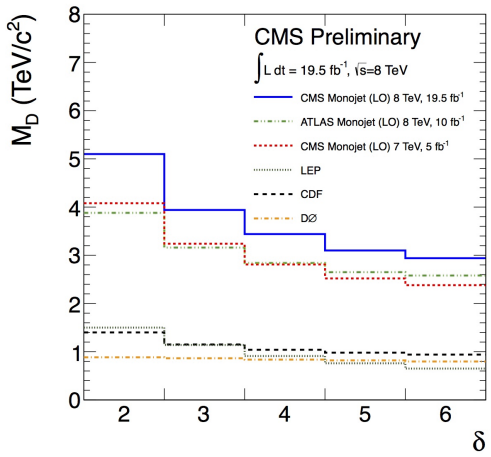

Fig. 2. Comparison of lower limits on M_D *versus* the number of extra dimensions with LEP, CDF, and D0 [4].

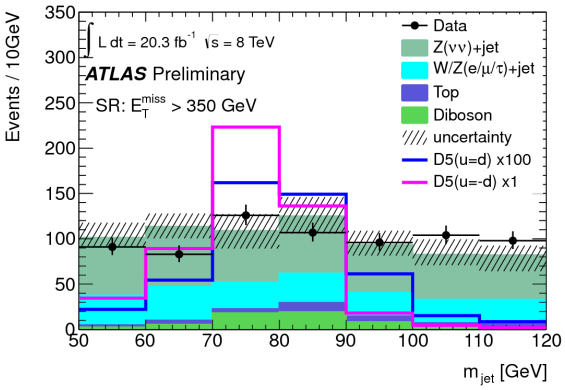

Fig. 3. Data and predicted background in the signal region $E_{\mathrm{T}}^{\mathrm{miss}} \geq 350$ GeV. Combined single W/Z boson signal distribution of D5 (effective operator for the spin-independent interaction model) destructive and D5 constructive case with dark matter mass of 1 GeV and $M_* = 1$ TeV are drawn as well. Uncertainties include statistical and systematic contributions [6].

Values of M_D below 3.88 TeV ($n = 2$), 3.16 TeV ($n = 3$), 2.84 TeV ($n = 4$), 2.65 TeV ($n = 5$) and 2.58 TeV ($n = 6$) are excluded at 95%. The observed limits decrease by 10% after considering the -1σ uncertainty from PDFs, scale variations, and parton shower modeling in the ADD theoretical

predictions. These results do not supersede the 95% C.L. limits obtained in the previous analysis based on 7 TeV data. The limits on M_D are not improved (except in the case of $n = 6$) due to the increase of the SM background levels and the lack of sufficient statistics in the MC samples employed for the background predictions.

ATLAS has carried out a search for dark matter pair production in association with a W or Z boson in pp collisions corresponding to 20.3 fb^{-1} of integrated luminosity at $\sqrt{s} = 8$ TeV. Events with large missing transverse momentum and a jet with mass consistent with a W or Z boson decay were analyzed. Figure 3 shows that data were consistent with the SM expectations, and limits were set on the mass scale in effective field theories, which describe the interaction of dark matter and SM particles [5, 6]. This analysis has reported the first LHC limits on dark matter production in events with a hadronically decaying W or Z boson and large missing momentum.

3. Searches with two leptons in the final state

The search with two leptons in the final state is rather straightforward. Benefits come from the careful study of objects and backgrounds. The aim of these analyses is to find two high-p_{T} leptons that are prompt and well-isolated, and to reconstruct the invariant mass of the resulting objects.

The benchmark model for Z' bosons is the Sequential Standard Model (SSM), in which the Z' (Z'_{SSM}) has the same couplings to fermions as the SM Z boson. A more theoretically-motivated model is a Grand Unification model in which the E_6 gauge group is broken into SU(5) and two additional U(1) groups. In this search, the resonances are assumed to have a narrow intrinsic width. The expected intrinsic width of the Z'_{SSM} as a fraction of its mass is 3.1%, while on any E_6 model the intrinsic width is predicted to be between 0.5% and 1.3% of its mass.

ATLAS and CMS are used to search for high mass resonances (Z') decaying to an electron–positron pair or a muon–antimuon pair. Results were presented from the analysis of pp collisions at a center-of-mass energy of 8 TeV corresponding to an integrated luminosity of approximately 20 fb^{-1}. The strategy was to search for narrow resonances in dimuon and dielectron invariant mass spectra. Figures 4 and 5 show that the spectra are consistent with expectations from the SM and upper limits have been set on the cross section times branching fraction for new boson production relative to the SM Z boson production.

A Z' with SM Z couplings to fermions was excluded at 95% C.L. for masses below 2.79 TeV in the electron channel, 2.48 TeV in the muon channel, and 2.86 TeV in the two channels combined. Limits on other model interpretations were also presented, including a Grand Unification model

based on the E_6 gauge group and a spin-2 Randall–Sundrum graviton [7]. CMS analysis excluded, at 95% C.L., a SSM Z'_{SSM} resonance lighter than 2.96 TeV and a superstring-inspired Z'_{ψ} lighter than 2.6 TeV. These are the most stringent limits to date [8].

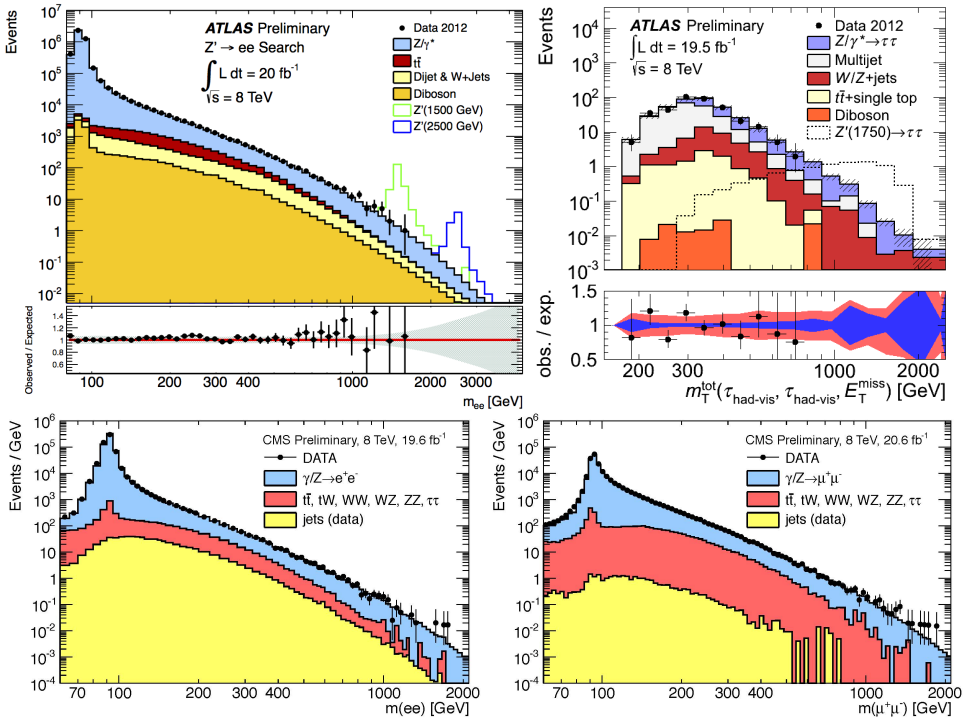

Fig. 4. Top: Dielectron invariant mass (m_{ee}) distribution (left) with statistical uncertainties after final selection, compared to the stacked sum of all expected backgrounds, with two selected Z' signals overlaid for ATLAS searches. The SSM bin width is constant in log m_{ee} [7]. In the lower part of the plot, the black points show the ratio of observed to expected events with statistical uncertainty, while the shaded band indicates the mass-dependent systematic uncertainty on the sum of the backgrounds. The $m_{\mathrm{T}}^{\mathrm{tot}}$ distribution after event selection in ditau searches (right) [9]. The estimated contributions from SM processes are stacked and appear in the same order as in the legend. A Z'_{SSM} signal with $m_{Z'} = 1.75$ TeV and the events observed in data are overlaid. Bottom: The invariant mass spectrum of ee (left) and $\mu^+\mu^-$ (right) events for CMS searches [8]. The points with error bars represent the data. The histograms represent the expectations from SM processes: Z/γ^*, $t\bar{t}$ and other sources of prompt leptons, and the multi-jet backgrounds. The Monte Carlo simulated backgrounds are normalized to the data in the region of $60 \leq m(ll) \leq 120$ GeV.

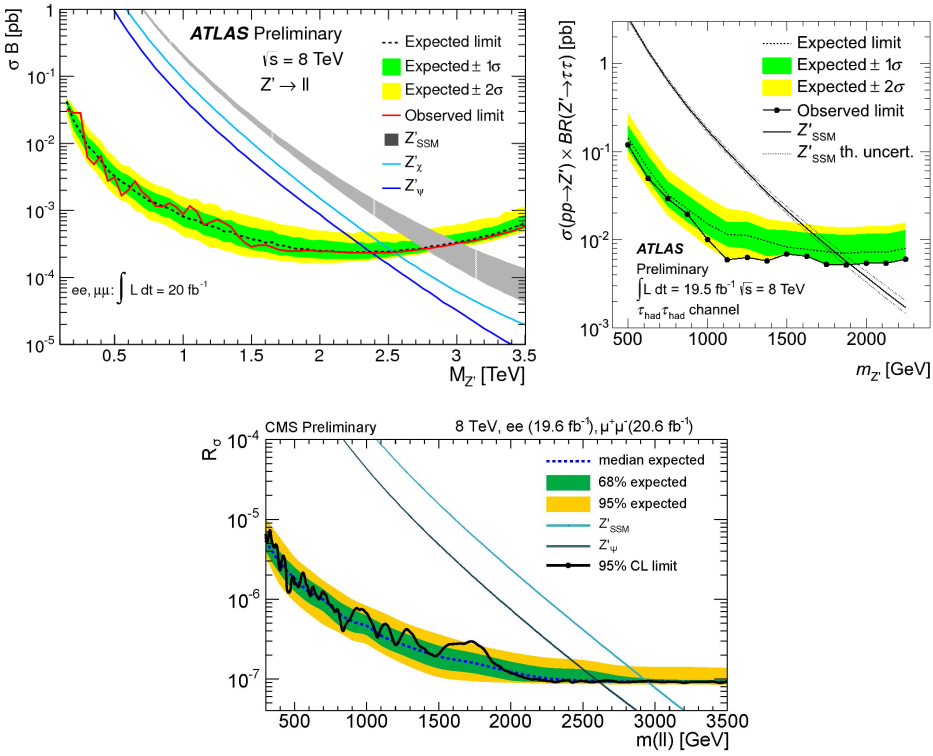

Fig. 5. Top left: Average expected (dashed line) and observed (solid/red line) 95% C.L. on σB, where B is the branching fraction, and expected σB for Z' production and the two E6-motivated Z' models with lowest and highest σB for the combination of the dielectron and dimuon channels in ATLAS searches [7]. The limits are conservative for E6-motivated Z' models due to their narrower intrinsic width. The inner and outer bands show the range in which the limit is expected to lie in 68% and 95% of pseudo-experiments, respectively. Top right: The thickness of the Z' SSM theory curve represents all theoretical uncertainties and holds for the other theory curves. Expected and observed 95% credibility upper limits including 1σ and 2σ uncertainty bands in ATLAS ditau searches [9]. Bottom: Upper limits as a function of resonance mass M on the production ratio R_σ of cross section times branching fraction into lepton pairs for Z_{SSM} and Z_ψ boson production to the same quantity for Z bosons for the combined dilepton final state in CMS searches. Shaded darker/green and lither/yellow bands correspond to the 68% and 95% quantiles for the expected limits [8].

A search for high-mass ditau resonances decaying in the fully hadronic final state has been performed. No statistically significant excess above the SM expectation was observed; 95% C.L. upper limits were set on the cross section times branching fraction of Z' resonances decaying into $\tau^+\tau^-$ pairs as a function of the resonance mass. As a result, Z' bosons of the SSM with masses below 1.90 TeV were excluded [9].

4. Searches with two jets in the final state

A search for new resonances and interactions in two-jet (dijet) final states, using the dijet mass distribution was presented using 2012 data with an integrated luminosity of 13.0 fb^{-1} (ATLAS) [10] and 19.6 fb^{-1} (CMS) [11]. The background was estimated using the observed dijet mass spectrum by fitting a smooth-four parameter function to the data

$$f(x) = p_1(1-x)^{p_2}x^{p_3+p_4\ln x}\,. \tag{1}$$

Jets were reconstructed using the anti-K_t jet clustering algorithm with the distance parameter, R, of 0.6. Events were selected where the two highest-p_T jets satisfy the rapidity requirement $|y| \leq 0.6$ and dijet mass criterion $m_{jj} \geq 1000$ GeV.

This treatment of the background greatly reduced the effects of jet energy scale uncertainties and the luminosity uncertainty. The search for new phenomena in the dijet mass distribution reduces to the search for significant local excesses ("bumps" or "resonances") above this parameterized background.

Figures 6 and 7 show that no resonance-like features have been observed in the dijet mass spectrum. A new 95% C.L. exclusion limit on the mass of excited quarks has been set at 3.84 TeV. Limits on $\sigma \times A$, where A is the acceptance, for simplified Gaussian resonances have also been extended from previous analysis [12, 13]. We set upper limits at the 95% confidence level on the resonance cross section. By comparing these generic limits with theoretical predictions for the cross section of several models of new particles, we set specific lower limits on the mass of string resonances, excited quarks, axigluons, colorons, s8 resonances, E_6 diquarks, W' and Z' bosons, and Randall–Sundrum gravitons. The lower mass limits reached up to 5.1 TeV, depending on the model, and extended previous exclusions [11].

The ATLAS Collaboration performed a search for a dijet resonance with an invariant mass in the range between 130 and 300 GeV in the processes $pp \to Wjj + X$ with $W \to l^{\pm}\nu$ and $pp \to Zjj + X$ with $Z \to l^+l^-$ ($l = e, \mu$) [14]. The data used correspond to 20.3 fb^{-1} of pp collisions at $\sqrt{s} =$ 8 TeV. The results shown in Fig. 8 were interpreted in terms of constraints on the Low Scale Technicolor model. No significant deviation from the

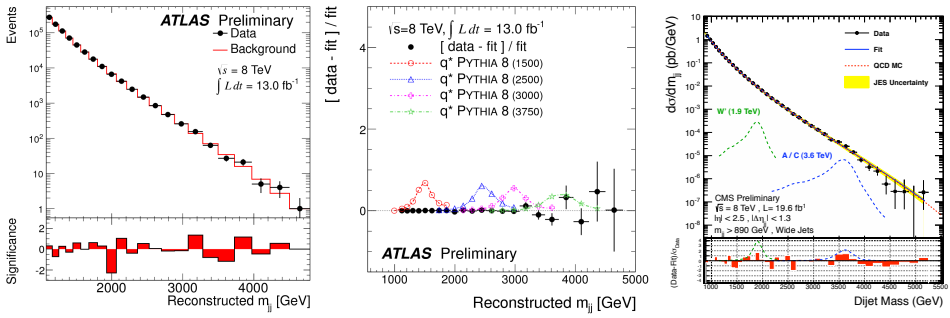

Fig. 6. Left: The reconstructed dijet mass distribution with statistical uncertainties (filled points with error bars) fitted with a smooth functional form (solid line). Middle: Four predicted excited quark (q^*) mass templates, normalized to the integrated luminosity, are compared to the data [10]. Right: Inclusive dijet mass spectrum from wide jets (points) compared to a smooth fit (solid) and predictions for QCD (short-dashed), W', axigluon/coloron (A/C). The shaded band shows the contribution from the systematic uncertainty in the jet energy scale [11].

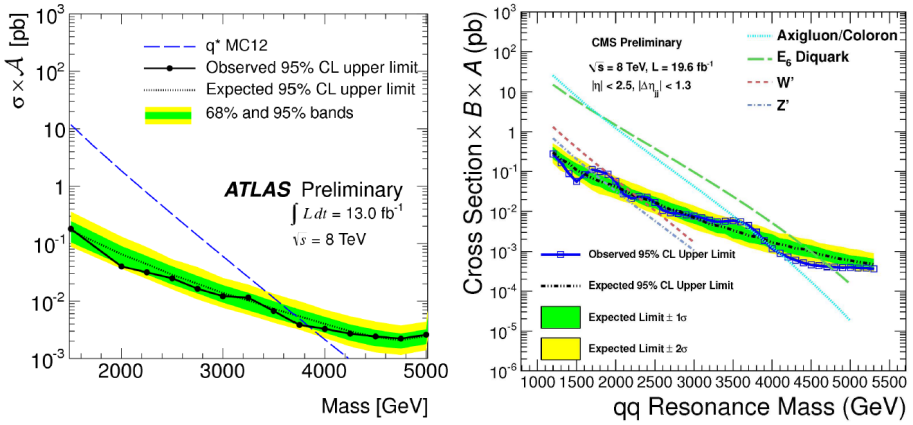

Fig. 7. Left: 95% C.L. upper limit on $\sigma \times A$ as a function of dijet resonance mass (black filled circles). The black dotted curve shows the expected 95% C.L. upper limit and the darker/green and lighter/yellow bands represent the 68% and 95% contours of the expected limit, respectively. The dashed/blue curve represents the excited-quark $\sigma \times A$ prediction [10]. Right: Observed 95% C.L. upper limits on $\sigma \times B \times A$ for quark–quark dijet resonances (points) are compared to the expected limits (dot-dashed) and their variation at 1σ and 2σ (shaded bands). Theoretical predictions for various resonance models are also shown [11].

SM background predictions was observed. Upper limits on the production cross section times branching fraction were set for a hypothetical technipion produced in association with a W or Z boson from the decay of a technirho particle.

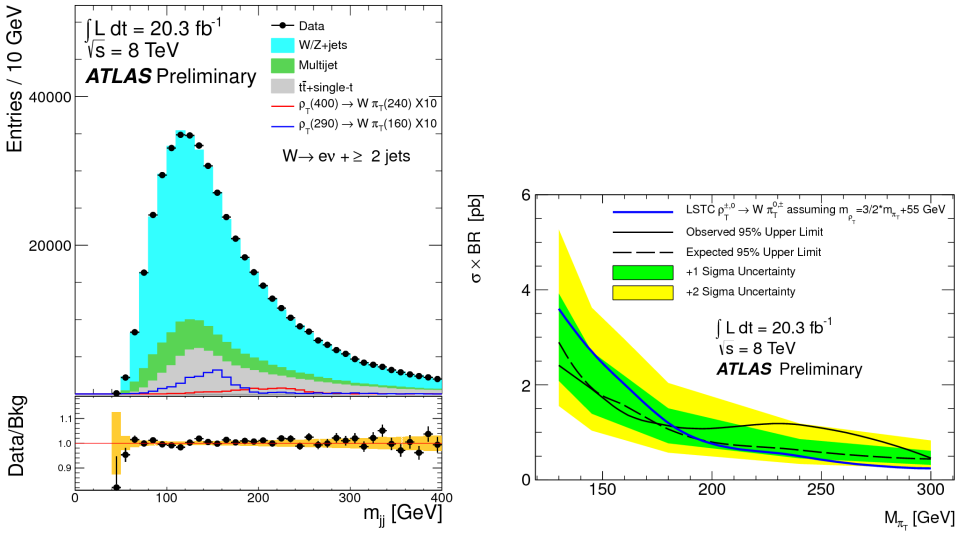

Fig. 8. Left: Fit to the dijet mass distribution of the expected background in the signal region for the Wjj channel with W to $e\nu$ and W to $\mu\nu$. The bottom part of the figure shows the ratio of data to fit result. Right: Observed and expected 95% C.L. upper limits on the technipion cross sections as a function of the mass of the technipion for the Wjj channel and the Zjj channel. The LSTC prediction for the ρ_{T} cross section are also shown [14].

5. Searches with $\gamma + X$ final states

Several exotic production mechanisms have been proposed that produce massive $\gamma +$ jet final states [15]. They include non-thermal quantum black holes (QBHS), excited quarks, *etc.* The analysis performed by the ATLAS Collaboration, described a model-independent search for $\gamma +$ jet production, improved the earlier search. It presented the first limits on QBHs decaying to the $\gamma +$ jet final state and placed new limits both on excited quarks and on a generic Gaussian-shaped source, which described other narrow resonant signals such as topological pions. Sensitivity to such signals was improved compared to the previous search through a combination of an order-of-magnitude larger data sample (20.3 fb^{-1}), a higher centre-of-mass energy ($\sqrt{s} = 8$ TeV), reduced background uncertainties, and improved selection criteria at high invariant mass.

Figure 9 shows the $\gamma + \text{jet}$ mass distribution compared to a background model fit from data; no significant deviation from the background-only hypothesis was found. Limits were set at 95% C.L. on generic Gaussian-shaped signals and two benchmark phenomena beyond the SM: non-thermal quantum black holes and excited quarks. Non-thermal quantum black holes were excluded below masses of 4.6 TeV and excited quarks were excluded below masses of 3.5 TeV.

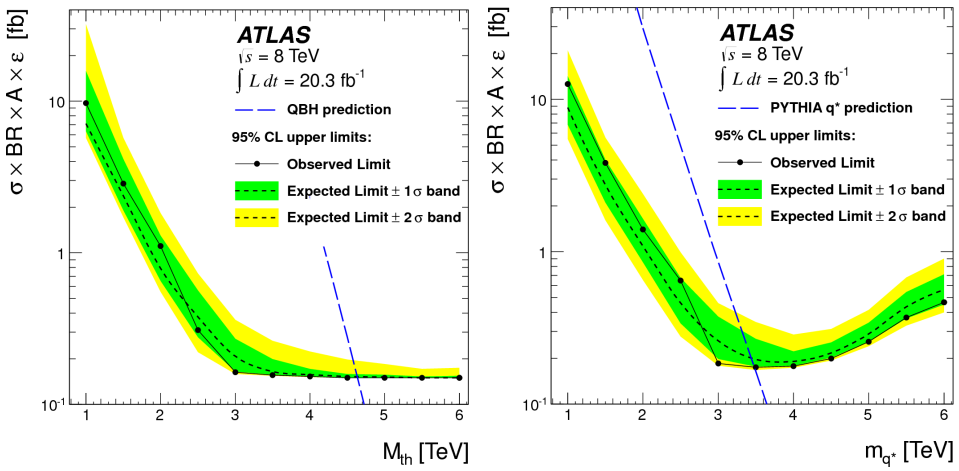

Fig. 9. Left: 95% C.L. upper limits on $\sigma \times \text{BR} \times A \times \epsilon$, where ϵ is the efficiency, for QBHs decaying to a γ and a jet, as a function of the threshold mass M_{th}, assuming $M_D = M_{\text{th}}$ and $n = 6$. The limits take into account statistical and systematic uncertainties. Points along the solid black line indicate the mass of the signal where the limit is computed. The black short-dashed line is the central value of the expected limit. The predicted visible cross section for QBHs is shown as the long-dashed line. Right: Same upper limits for excited quarks decaying to a γ and a jet, as a function of the signal mass m_{q^*}. The long-dashed line shows the predicted visible cross section for excited-quark production from Pythia [15].

Compositeness models could explain the source of the mass hierarchy and the generational structure of quarks and leptons [16]. Compositeness models address these questions by proposing that quarks and leptons are composed of hypothetical constituents usually referred to as preons. In these models, quarks and leptons are the lowest-energy bound states of these hypothetical particles. New interactions among quarks and leptons should then be visible at the scale of the constituents binding energies and give rise to excited states. At the LHC, excited lepton l^* production via four-fermion contact interactions has been searched.

Previous searches at LEP, HERA, and the Tevatron have found no evidence for such excited leptons. Figure 10 shows the case where $\Lambda = m_l^*$ (where Λ is the compositeness scale), e^* and μ^* masses below 2 TeV have been excluded at the 95% C.L. based on the study of 5 fb^{-1} of data recorded at $\sqrt{s} = 7$ TeV by the ATLAS and CMS experiments.

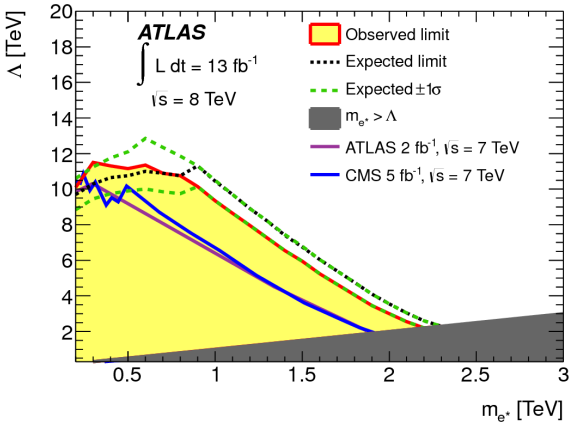

Fig. 10. Exclusion limit in the compositeness scale (Λ) *vs.* excited-lepton mass (m_l^*) parameter space for the electron channel. The filled area is excluded at 95% C.L. No limits are set in the dark shaded region $m_l^* \geq \Lambda$ where the model is not applicable [16].

5.1. More on black holes

A search for quantum black-hole production using 20.3 fb^{-1} of ATLAS data at $\sqrt{s} = 8$ TeV has been performed [17]. Quantum black holes are assumed to decay into a lepton (electron or muon) and a jet. In either channel, no event with a lepton–jet invariant mass of 3.5 TeV or more was observed, consistent with the expected background. Limits were set on the product of cross sections and branching fractions for the lepton+jet final states of quantum black holes produced in a search region for invariant masses above 1 TeV. The combined 95% C.L. upper limit on this product for quantum black holes with threshold mass above 3.5 TeV was 0.18 fb. This limit constrains the threshold quantum black-hole mass to be above 5.3 TeV in the model considered.

With the same data, the ATLAS Collaboration carried out a search for microscopic black holes in a like-sign dimuon final state. Using a high track multiplicity requirement, 0.6±0.2 background events from SM processes were predicted and none observed. This result was interpreted in the context of low-scale gravity models and 95% C.L. lower limits on microscopic black holes masses were set for different model assumptions [18].

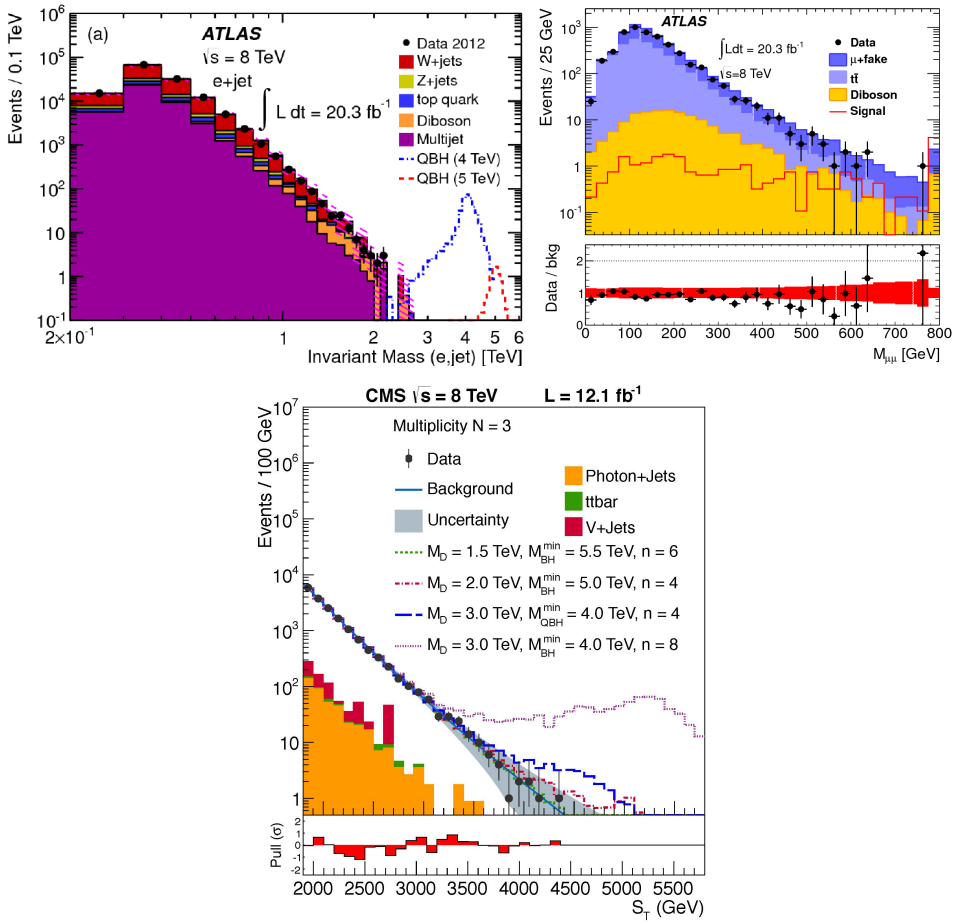

Fig. 11. Top left: Distribution of the invariant mass of the lepton and highest-p_{T} jet in the electron+jet channel, for data (points with error bars) and for SM backgrounds (solid histograms) [17]. Top right: The dimuon invariant mass distribution for the predicted background and observed data for like-sign dimuon events where the leading muon satisfies $p_{\mathrm{T}} \geq 1004$ GeV [18]. Bottom: Total transverse energy S_{T}, for events with the multiplicity $N = 3$ objects in the final state. Data are depicted as solid circles with error bars; the shaded band is the background prediction obtained from data (solid line) with its uncertainty [19].

The CMS Collaboration performed a search for microscopic black holes and string balls based on a data sample of pp collisions at $\sqrt{s} = 8$ TeV with an integrated luminosity of 12 fb^{-1}. No excess of events with energetic multiparticle final states, typical of black hole production or of similar new physics processes, was observed. Given the agreement of the observations with the expected SM background, which is dominated by QCD multi-jet

production, 95% C.L. limits were set on the production of semiclassical or quantum black holes, or of string balls, corresponding to the exclusion of masses below 4.3 to 6.2 TeV, depending on model assumptions. In addition, model-independent limits (on the production cross section) were set on new physics processes resulting in energetic multiparticle final states [19].

To extract the upper limit on the lepton+jet cross section, a fit to the invariant mass distribution was performed as it is shown in the left panel of Fig. 11. No event with a lepton+jet invariant mass of 3.5 TeV or more was observed. Therefore, the limits on QBH mass have been set to be above 5.3 TeV. For the dimuon invariant mass analysis shown in the middle plot of Fig. 11, the bottom panel shows the ratio of data to the expected background (points) and the total uncertainty on the background (shaded area). No excess of events was observed over the SM background. In the case with energetic multi-particle final states, the predicted semi-classical (quantum) black hole signal for three different (one) parameter sets are shown in the right plot of Fig. 11. The bottom panel shows the pull distribution based on combined statistical and systematic uncertainty (dominated by the latter). Masses below 4.3 to 6.2 TeV were excluded.

6. Searches with diboson in the final state

The search for diboson resonances is a sensitive probe of the mechanism of electroweak symmetry breaking (EWSB) [20]. Such resonances can be, besides the SM Higgs boson, new states predicted by scenarios beyond the SM such as a technirho and other technimesons in Technicolor models, or a new heavy gauge boson in composite Higgs models, or Little Higgs models. A simple benchmark model conventionally used is the extended gauge model (EGM), where a W' has the same fermionic couplings as the W boson of the SM but the triple gauge coupling $W'WZ$ is suppressed with respect to that of the SM, such that its width remains proportional to its mass.

In this search, we have in the final state a charged resonance decaying to WZ with the subsequent decays of both W and Z involving charged leptons ($l = e, \mu$) and one neutrino. The dataset used corresponds to an integrated luminosity of 13 fb^{-1}, collected by ATLAS in pp collisions at a center-of-mass energy of $\sqrt{s} = 8$ TeV during the 2012 run. Two benchmark models were used to interpret the results: the EGM with a heavy W' boson, and the Low Scale Technicolor (LSTC) model. Searches for the EGM W' in the WZ channel have been performed at the Tevatron and have excluded W' bosons with a mass between 180 GeV and 690 GeV at 95% C.L. The CMS experiment has searched for EGM W' bosons, excluding masses below 1143 GeV. The ATLAS experiment has searched for the same bosons and no significant localized excess was observed in the reconstructed WZ invariant mass distribution as it is shown in Fig. 12. Upper limits on the production

cross section times branching ratio were derived and bounds on the resonant mass were obtained in the context of benchmark EGM and LSTC models. Figure 12 (right) shows that at 95% C.L., EGM W' bosons with masses up to 1180 GeV were excluded. Assuming the kinematics of the W' production and decay are valid for the ρ_{T} technimeson, ρ_{T} with masses up to 920 GeV were excluded.

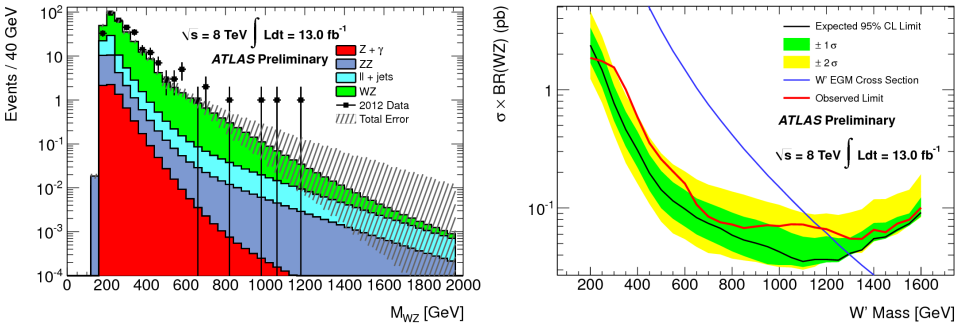

Fig. 12. Left: Comparison of the data with the background estimation for events with all selection cuts applied and including extrapolated background: WZ bosons invariant mass with liner and log scale. Right: The expected excluded production cross section limit at 95% C.L. multiplied by the branching fraction for the combined $e\nu$, ee, $\mu\nu ee$, $e\nu\mu\mu$, and $\mu\nu\mu\mu$ final state assuming the $W' \to WZ$ signal [20].

Another analysis performed by ATLAS is the search for a new narrow resonance decaying to a ZZ boson pair, where one Z boson decays leptonically and the other decays hadronically (denoted as $llqq$ final state) or decaying to W/Z bosons with the subsequent decays into leptons and quarks, characterized by the presence of high-p_{T} leptons and jets in the final state [21]. The benefit of semi-leptonic final states is the reduction of multi jet background with respect to the fully hadronic states, while preserving the larger hadronic decay branching ratio.

This search used a data sample corresponding to 7.2 fb^{-1} collected by the ATLAS experiment at $\sqrt{s} = 8$ TeV. The results were interpreted based on a spin-2 Randall–Sundrum (RS) Graviton (G^* decaying to a ZZ pair, in the context of the "bulk RS model" in which the fermion and boson fields of the SM are free to propagate into the extra dimension). Figure 13 (left) shows that no significant deviation in the mass distribution from a smoothly falling background distribution was observed. Upper limits on the production cross section times branching fraction into a ZZ boson pair were set for the bulk RS graviton with coupling parameter $K/\overline{m}_{\mathrm{Pl}} = 1.0$, and the corresponding 95% C.L. observed (expected) lower limit on the mass for the graviton was 850 GeV.

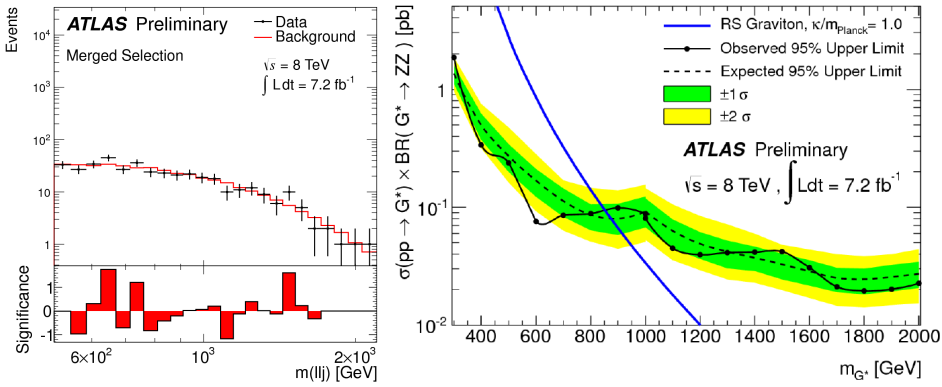

Fig. 13. Left: Distribution of reconstructed m_{llj} in the merged signal region for the combined electron and muon channels, shown for data and background. The variable bin sizes are used to match the resolution of reconstructed resonance masses. The local deviation of the data from the background expectation is also shown and takes into account statistical uncertainties only. Right: Observed and expected 95% credibility level upper limits on $\sigma(pp \to G^* \times)\mathrm{BR}(G^* \to Z)$ for the bulk RS graviton with a coupling of $\kappa/m_{\mathrm{Pl}} = 1.0$. The LO theoretical prediction for the bulk RS model is also shown. The inner and outer bands on the expected limit represent 1σ and 2σ variations, respectively [21].

The CMS Collaboration performed a search for high-mass resonances decaying to WW in the final states with one $W \to l\nu(l = e, u)$ [22] and the other W decaying hadronically. Such processes are prominent features of several extensions of the SM. For example, compositeness models predict the existence of scalar or vectorial resonances coupling to a pair of vector bosons. Similarly, the branching fraction of a RS graviton to WW is enhanced if the graviton is allowed to propagate in the bulk. The analysis was based on pp collisions data at $\sqrt{s} = 8$ TeV during 2012, corresponding to an integrated luminosity of 19.5 fb^{-1}. The signal is characterized as a local enhancement in the WW invariant mass distribution. Jet substructure techniques were exploited for separating the signal from the SM background when the boost of the W causes the two quarks to merge into the same jet reconstructed in the detector. Two different background estimate techniques were used providing consistent results.

Figure 14 shows that no significant excess above the expected background was found. Upper limits at 95% C.L. on the bulk graviton production cross section times branching ratio to WW were set in the range from 70 fb to 3 fb for resonance masses between 0.8 and 2.5 TeV, respectively.

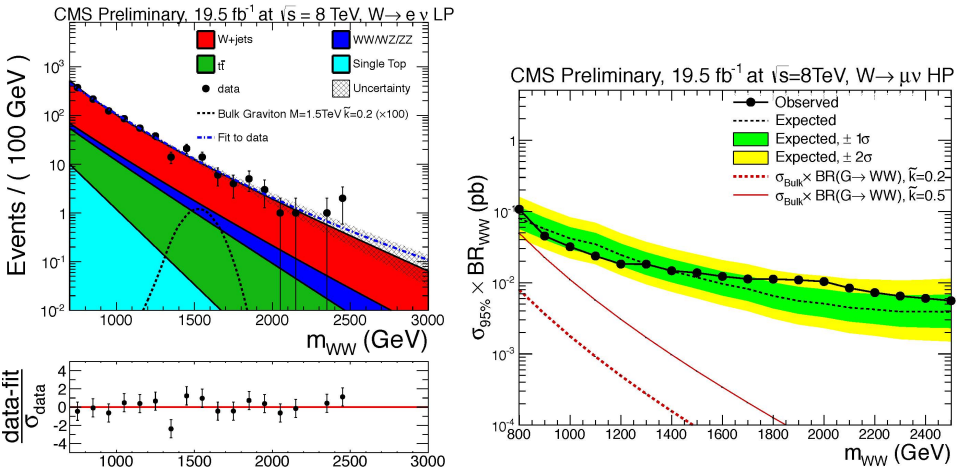

Fig. 14. Left: Final distributions in m_{WW} for data and expected background. Fit to the signal mass distribution, using a Crystal Ball function is also shown for a bulk graviton with mass of 1.5 TeV and $\kappa = 0.2$ (coupling constant). The dashed/blue line is the fit to data (cross-check method). Right: Limit for muon category. Observed (dashed) and expected (solid) 95% C.L. upper limit on bulk graviton production cross section times the branching fractions of $G \to WW$ using 19.5 fb^{-1} of data. The limit is obtained with the Asymptotic CLs technique. The expected product of the bulk graviton production cross section and the branching fraction is shown as a dashed (solid)/red curve for $\kappa = 0.2$ ($\kappa = 0.5$) [22].

7. Searches for $t\bar{t}$ resonances

The ATLAS experiment searches for the production of top quark pair ($t\bar{t}$) resonances produced in pp collisions at $\sqrt{s} = 8$ TeV using a data set collected in 2012 with an integrated luminosity of 14.3 fb^{-1}. The search was carried out in the lepton plus jets decay channel where, one W boson from a top quark decays leptonically and the other decays hadronically. The $t\bar{t}$ invariant mass spectrum was tested for any local excess of events that may result from a resonance decaying to $t\bar{t}$. It was reconstructed using a combination of *resolved* and *boosted* reconstruction methods [23]. Using the former, the hadronically decaying top quark was identified by two or three distinct small-radius jets. Using the latter, the hadronically decaying top quark was identified by one large-radius jet that had substructure consistent with being composed of the decay products of a W boson and a b quark. High momentum top quark decays were reconstructed more efficiently using the boosted reconstruction technique. The semileptonically decaying top quark was identified by a lepton, one small radius jet and missing transverse momentum.

The CMS top pair production signatures are classified based on whether the W bosons decay to leptons or quarks, since the top quark decays primarily to a W boson and a bottom quark [24]. This measurement combines analyses utilizing the final states where one or both W bosons from $t\bar{t}$ events decay to quarks ("semileptonic" and "all-hadronic" events, respectively). The events are classified into two categories based on the expected kinematics of the top-quark decay products. In the first category, the $t\bar{t}$ pair is produced near the kinematic threshold, resulting a topology where each parton is matched to a single jet. In the second category, each top quark is produced with a high Lorent boost, resulting in collimated decay products that may be clustered into a single jet ("boosted topology").

Experiments at the LHC have used two specific theoretical models as benchmarks. The models test the production of resonances with both narrow and broad widths relative to the detector resolution which is of the order of 7%. The narrow resonance benchmark is a topcolor, leptophobic Z' resonance. Identical model parameters were used by the D0 and the CDF collaborations including a resonance width of $\Gamma_{Z'}/m_{Z'} = 1.2\%$. The broad resonance benchmarks are Kaluza–Klein (KK) gluons that arise in Randall–Sundrum models with an extra dimension with a warped geometry and where all the SM fields and matter can propagate in all five dimensions. A resonance width of $\Gamma_{gKK}/m_{gKK} = 15.3\%$ was used.

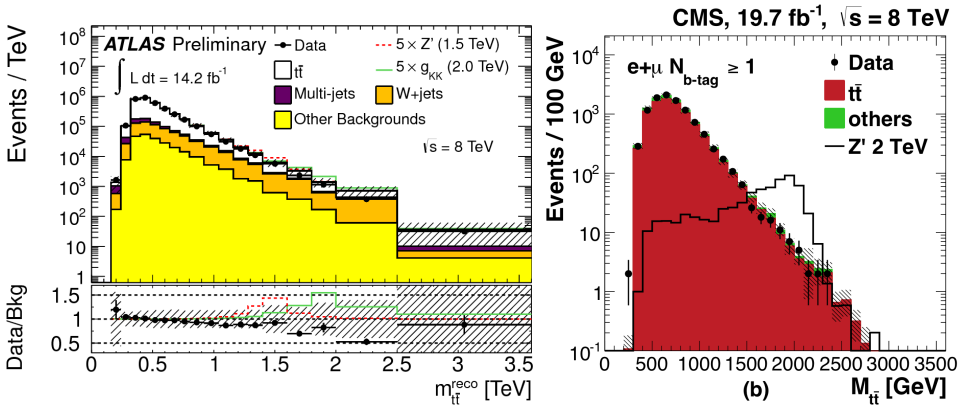

Fig. 15. Left: The $t\bar{t}$ invariant mass spectrum, summing the spectra from the two channels and the two selection methods. The shaded areas indicate the total systematic uncertainties. Two benchmark signals are indicated on top of the background, a Z' with $m = 1.5$ TeV and a g_{KK} with $m = 2.0$ TeV [23]. Right: Comparison between data and SM prediction for reconstructed $t\bar{t}$ invariant mass distributions for the boosted semi-leptonic analysis with at least 1 b-tagged jet [24, 25].

The best CMS limits at 95% C.L. on the benchmark resonances came from a search using data taken at $\sqrt{s} = 8$ TeV with integrated luminosity of 20 fb^{-1} [24, 25]. Figure 15 shows both for ATLAS and CMS that no evidence for a $t\bar{t}$ resonance was found and 95% C.L. limits on the production rate were determined for massive states using both benchmark models. Figure 16 shows that the expected lower mass limits for this CMS search was 2.0 TeV for the leptophobic top color Z'. The expected lower mass limits found for the KK gluon was 2.2 TeV. Figure 16 shows also the results found by ATLAS. The upper limits on the cross section times branching ratio of a narrow Z' boson decaying to top pairs range from 5.3 pb for a resonance mass of 0.5 TeV to 0.08 pb for a mass of 3 TeV. A narrow leptophobic top color Z' boson with a mass below 1.8 TeV was excluded by ATLAS. Upper

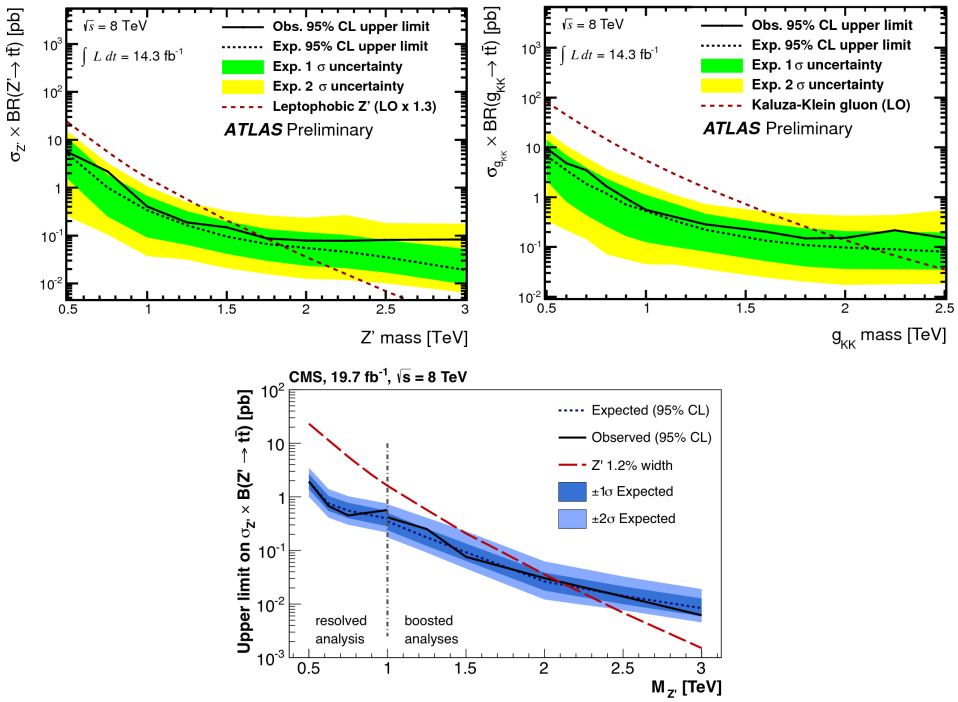

Fig. 16. Top left: Observed and expected upper cross section limits times the $t\bar{t}$ branching ratio on a Z' bosons. The resolved and the boosted selections have been combined in the estimation of the limits. Both systematic and statistical uncertainties are included [23]. Top right: Observed and expected upper cross section limits times the $t\bar{t}$ branching ratio on a Kaluza–Klein gluons [23]. Bottom: The 95% C.L. upper limits on the production cross section times branching fraction as a functions of $t\bar{t}$ invariant mass for Z' resonances with $\Gamma_{Z'}/m_{Z'} = 1.2\%$ compared to theory predictions [24, 25].

limits were set on the cross section times branching ratio for a broad KK gluon with $\Gamma_{gKK}/m_{gKK} = 15.3\%$ decaying to $t\bar{t}$. A KK gluon was excluded for masses below 2.0 TeV by ATLAS.

8. Searches for vector-like top quarks

The discovery of a light particle consistent with the Higgs boson raises the question for a mechanism to stabilize the mass of this particle. Loop corrections to the mass of a scalar particle diverge quadratically with the cut-off scale of the calculations. The dominant contribution arise from loops that involve top quarks, W bosons, and Higgs bosons. If the SM applies to energies significantly above the electroweak scale, there must be other new particles that give rise to loop corrections that cancel these contributions. Little Higgs models, for example, predict the existence of a partner quark T to the top quark that would cancel the contributions of the top quark loops to the Higgs boson mass [26]. This T quark must have a mass at or below the TeV scale if it is to effectively fulfill this role. In these searches, we assume that the T quark has only vector couplings with the W and Z bosons and that it is an electroweak singlet, thereby evading the many constants that precision electroweak measurements place on fourth generation quarks in the framework of the SM.

We assume that the T quark is pair produced together with its antiquark in proton–proton collisions through the strong interaction. Thus its productions cross section can be calculated using perturbative QCD. According

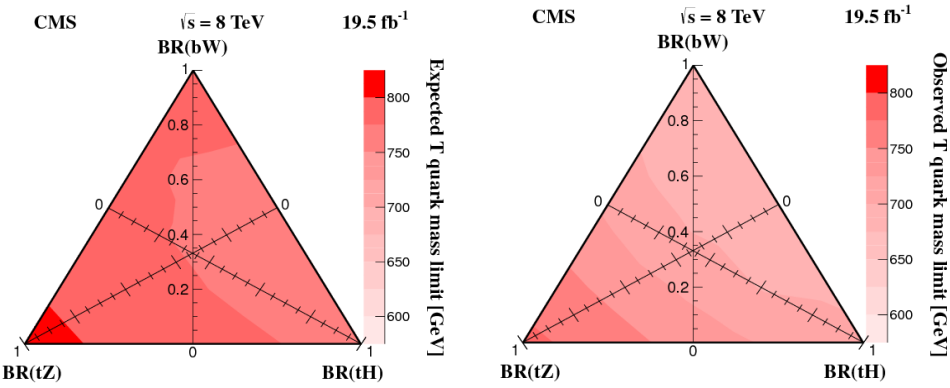

Fig. 17. Branching fraction triangle with expected limits (left) and observed limits (right) for the T quark mass. Every point in the triangle corresponds to a particular set of branching fractions values subject to the constraint that all three add up to one. The branching fraction for each mode decreases from one at the corner labeled with the decay mode to zero at the opposite side of the triangle [26].

to the approximate next-to-next-to-leading order calculation the $T\overline{T}$ production cross section varies from 570 to 3.3 fb for T quark masses between 500 GeV and 1 TeV. Such a T quark can decay into three different final states: bW, tZ or tH. If the decay is democratic, then the branching fractions should be 50% into bW and 25% each into tZ and tH.

ATLAS and CMS search for the T quark signal independently of its specific branching fractions. Searches have considered three final states.

The CMS assumption is that the T quark decays exclusively into bW, tZ, and tH and select events with at least one isolated lepton, lower limits are set for T mass between 687 and 782 GeV for all possible branching fractions into these three final states. This was the first search that considered all three final states and the limits place the most stringent constraints on the existence of such a quark so far. The resulting lower limits for the T quark mass are represented graphically in Fig. 17 for the CMS search. The data were accumulated by the CMS at the LHC in 2012 at $\sqrt{s} = 8$ TeV and correspond to an integrated luminosity of 19.6 fb^{-1}.

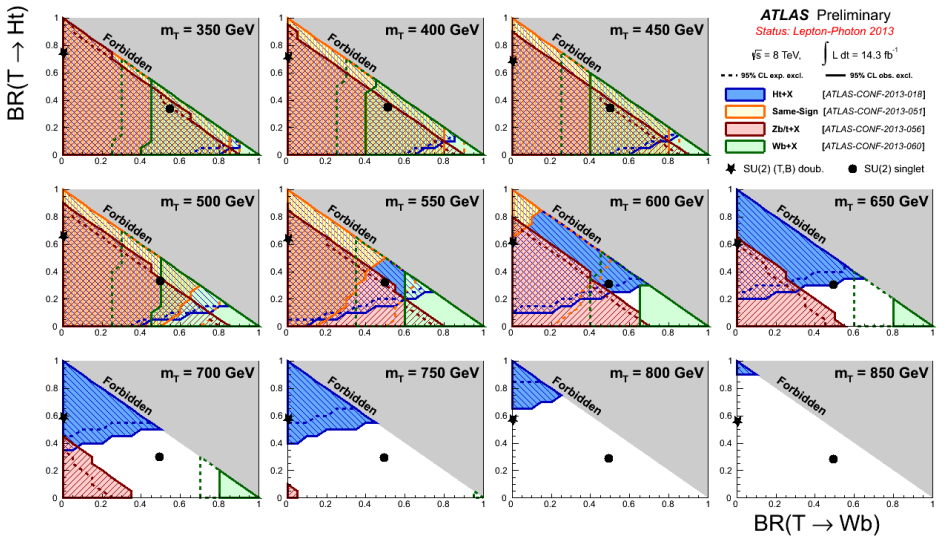

Fig. 18. Observed (filled area) and expected (dashed line) 95% C.L. exclusion in the plane of BR($T \to Wb$) *versus* BR($T \to Ht$), for different values of the vector-like top-quark mass. The dark shaded/gray area corresponds to the unphysical region where the sum of branching ratios exceeds unity. The default branching ratio values for the weak-isospin single and doublet cases are shown as plain circle and star symbols, respectively. This results includes both statistical and systematic uncertainties [27–30].

ATLAS searches for vector-like T quarks with 14 fb^{-1} of 8 TeV data. Figure 18 shows the excluded regions which are drawn sequentially for each of the analyses (bW, tZ or tH) in chronological order and overlaid (rather than combined) in each of the plots. This figure shows all four limits for the vector-like T quark. ATLAS has full coverage up to 550 GeV considering all three final states [27–30].

9. Conclusions

The excellent performance of the LHC and of the ATLAS and CMS detectors allowed our collaborations to perform high-quality studies in Exotic Physics. We reviewed some of the most recent results. The data collected by the experiments in 2012 allowed to exclude wide ranges of masses and production cross sections of many different exotic particles. No deviation from the SM has been found yet, but there are more boxes still to open at 8 TeV and we are very excited for the 13 TeV run in 2015 where a wider space parameter will be explored. Figure 19 shows ratios of LHC parton luminosities: 13 TeV/8 TeV. The ratio gives an idea of how much the sensitivity will improve at high energies.

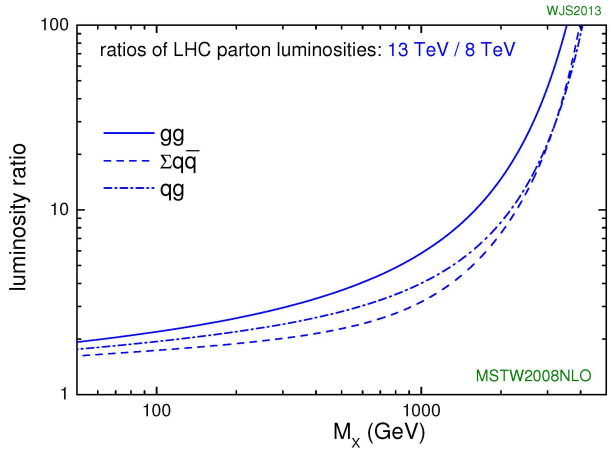

Fig. 19. Ratios of LHC parton luminosities: 13 TeV/8 TeV.

REFERENCES

[1] ATLAS Collaboration, *JINST* **3**, S08003 (2008).
[2] CMS Collaboration, *JINST* **3**, S08004 (2008).
[3] ATLAS Collaboration, ATLAS-CONF-2012-147.
[4] CMS Collaboration, PAS EXO12048.
[5] ATLAS Collaboration, ATLAS-CONF-2013-073.
[6] ATLAS Collaboration, *Phys. Rev. Lett.* **112**, 041802 (2014) [arXiv:1309.4017 [hep-ex]].
[7] ATLAS Collaboration, ATLAS-CONF-2013-017.
[8] CMS Collaboration, PAS EXO12061.
[9] ATLAS Collaboration, ATLAS-CONF-2013-066.
[10] ATLAS Collaboration, ATLAS-CONF-2012-148.
[11] CMS Collaboration, PAS EXO12059.
[12] ATLAS Collaboration, ATLAS-CONF-2012-088.
[13] CMS Collaboration, PAS EXO12016.
[14] ATLAS Collaboration, ATLAS-CONF-2013-074.
[15] ATLAS Collaboration, *Phys. Lett.* **B728**, 562 (2013).
[16] ATLAS Collaboration, ATLAS-CONF-2012-146.
[17] ATLAS Collaboration, arXiv:1311.2006 [hep-ex].
[18] ATLAS Collaboration, *Phys. Rev.* **D88**, 072001 (2013).
[19] CMS Collaboration, *J. High Energy Phys.* **07**, 178 (2013).
[20] ATLAS Collaboration, ATLAS-CONF-2013-015.
[21] ATLAS Collaboration, ATLAS-CONF-2012-150.
[22] CMS Collaboration, PAS EXO12021.
[23] ATLAS Collaboration, ATLAS-CONF-2013-052.
[24] CMS Collaboration, *Phys. Rev. Lett.* **111**, 211804 (2013).
[25] CMS Collaboration, CMS-PAS-B2G-12-006.
[26] CMS Collaboration, *Phys. Lett.* **B729**, 149 (2014).
[27] ATLAS Collaboration, ATLAS-CONF-2013-018.
[28] ATLAS Collaboration, ATLAS-CONF-2013-051.
[29] ATLAS Collaboration, ATLAS-CONF-2013-056.
[30] ATLAS Collaboration, ATLAS-CONF-2013-060.